

Three component model of cosmic ray spectra from 10 GeV to 100 PeV

V. I. Zatsepin and N. V. Sokolskaya

Skobeltsyn Institute of Nuclear Physics, Moscow State University, Russia
e-mail: viza@dec1.sinp.msu.ru

Received 28 February 2006 / Accepted 21 April 2006

ABSTRACT

Aims. A model to describe cosmic ray spectra in the energy region from 10^{10} to 10^{17} eV is suggested based on the assumption that Galactic cosmic ray flux is a mixture of fluxes accelerated by shocks from nova and supernova of different types.

Methods. We analyze recent experimental data on cosmic ray spectra obtained in direct measurements above the atmosphere and data obtained with ground extensive air shower (EAS) arrays.

Results. The model of the three classes of cosmic ray sources is consistent with direct experimental data on cosmic ray elemental spectra and gives a smooth transition from the all particle spectrum measured in the direct experiments to the all particle spectrum measured with EAS.

Key words. cosmic rays – ISM: supernova remnants – ISM: abundances

1. Introduction

It is thought that cosmic rays below 10^{17} eV are accelerated by shocks of supernova explosions, with all components having the same rigidity spectra. However, recent experimental data show that spectral indices of elemental spectra are different. Therefore we suggest that the concept of a single population of sources with the same index of rigidity spectra for all elements is inaccurate. We describe the experimental data using the idea that the measured cosmic ray flux is generated by three different classes of sources. It is suggested that each class of sources generates the spectrum that is power-law by rigidity with its specific spectral index and maximal rigidity. We analyze cosmic ray spectra, measured by direct methods, and all-particle spectra, measured in the extensive air showers (EAS). The data used are shown in Table 1.

2. Basis for the model

The model is based on the preliminary experimental data obtained in the ATIC-2 experiment (Wefel et al. 2005; Panov et al. 2006; Batkov et al. 2005) that fill the gap between measurements with magnetic spectrometers below 100 GeV (Haino et al. 2004; Alcaraz et al. 2000a,b; Boezio et al. 2003) and emulsion experiments above 10 TeV (Zatsepin et al. 1994; Asakimori et al. 1998; Derbina et al. 2005). The proton and helium spectra obtained in these direct measurements are shown in Fig. 1. The preliminary ATIC-2 data show that the proton spectrum obeys a power law with a spectral index of $\gamma = 2.63 \pm 0.01$ in the energy region between 3×10^2 and 10^4 GeV. However, the extrapolation of this spectrum to higher energy does not agree with the emulsion experiment data. Let us suppose that this difference is real, and that we see the end of acceleration for the first class of sources, while sources of the second class accelerate cosmic rays efficiently up to the knee region at about 3×10^{15} eV. Initially we suppose that the steeper spectrum below 3×10^2 GeV is connected with weak

reacceleration of cosmic rays during their propagation from the sources to the Earth. The helium spectrum is flatter than the proton one. This difference may be explained by the assumption that the second type of sources has a different spectral index, and that the elemental composition for these two classes of sources are different.

3. Description of the model

The equilibrium spectra in the Galaxy will be described in the framework of the Leaky Box model:

$$I(R) = \frac{Q(R) \times \tau_{\text{esc}}(R)}{1 + \lambda_{\text{esc}}(R)/\lambda_p}, \quad (1)$$

where R is the particle rigidity, $Q(R)$ is the source spectrum, τ_{esc} is the cosmic ray life time for the escape, λ_p is the particle mean free path for interaction, and λ_{esc} is the escape length ($\lambda_{\text{esc}}(R) = \rho \times v \times \tau_{\text{esc}}(R)$, where ρ is the density of the interstellar medium and v is the particle velocity).

The Leaky Box model without reacceleration adequately describes the spectra of nuclei and the ratios of secondary nuclei to primary ones in the HEAO-3-C2 experiment below 35 GeV/nucleon (Engelmann et al. 1990), if

$$\lambda_{\text{esc}}(R) = 34.1 \times R^{-0.6} \text{ g/cm}^2 \quad \text{for } R \geq 4.4 \text{ GV} \quad (2)$$

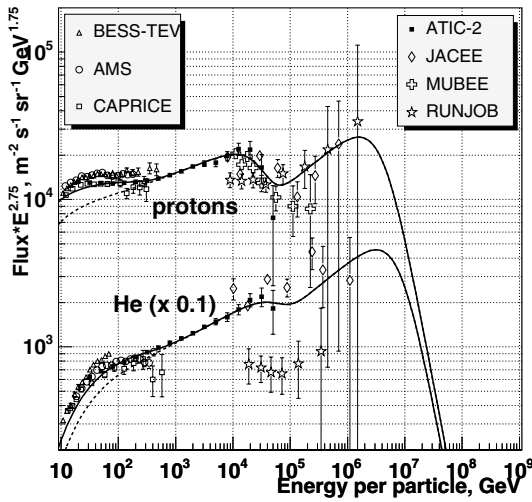
$$\lambda_{\text{esc}}(R) = 10.8 \times \beta, \text{ g/cm}^2 \quad \text{for } R < 4.4 \text{ GV}$$

$$\text{and } Q(R) \sim R^{-2.23};$$

but we assume that at high energy $\lambda_{\text{esc}}(R) \sim R^{-1/3}$, that corresponds to the Kolmogorov type of magnetic turbulence, and that the dependence in Eq. (2) at $R < 100$ GV results from reacceleration of cosmic rays during their propagation in the Galaxy.

Table 1. Experiments used in this paper.

Experiment	Technique	Site	Reference
AMS	Magnetic spectrometer	Spacecraft	Alcaraz et al. (2000a,b)
CAPRICE	Magnetic spectrometer	Balloon	Boezio et al. (2003)
BESS-TEV	Magnetic spectrometer	Balloon	Haino et al. (2003)
ATIC-2	Calorimeter	Balloon	Wefel et al. (2005); Panov et al. (2006)
SOKOL	Calorimeter	Spacecraft	Ivanenko et al. (1993)
JACEE	Emulsion chamber	Balloon	Asakimori et al. (1998); Takahashi et al. (1998)
MUBEE	Emulsion chamber	Balloon	Zatsepin et al. (1993, 1994)
RUNJOB	Emulsion chamber	Balloon	Derbina et al. (2005)
HEAO	Čerenkov counter	Spacecraft	Engelmann et al. (1990)
CRN	Transition radiation	Spacecraft	Müller et al. (1991)
TRACER	Transition radiation	Balloon	Müller et al. (2005)
TIC	Calorimeter	Balloon	Adams et al. (1997)
KASCADE	EAS	Ground based	Roth et al. (2003)
HEGRA-AIROBIC	EAS+Čerenkov light	Ground based	Arqueros et al. (2000)
CASA-BLANCA	EAS+ Čerenkov light	Ground based	Fowler et al. (2000)
DICE	Čerenkov light	Ground based	Kieda et al. (1999)
TUNKA	Čerenkov light	Ground based	Budnev et al. (2005)

**Fig. 1.** Proton and He spectra. Dashed lines are described in Sect. 3, solid lines are described in Sect. 5.

According to Osborne & Ptuskin (1988) reacceleration may be taken into account as follows:

$$\lambda_{\text{esc}}(R) = 4.2 \times (R/R_0)^{-1/3} \times [1 + (R/R_0)^{-2/3}] \text{ g/cm}^2, \quad (3)$$

where $R_0 = 5.5$ GV. It is assumed that

$$Q(R) \sim R^{-\alpha} \times \phi(R), \quad (4)$$

where α is the index of the source spectrum, and the function $\phi(R)$ describes smooth transition from the spectral index in the region of effective acceleration for each type of source to the spectral index after termination of this process.

$$\phi(R) = [1 + (R/R_{\text{max}})^2]^{(\gamma - \gamma_k)/2} \quad (5)$$

where $\gamma = \alpha + 0.33$ is the spectral index in the region of effective acceleration (at high enough energy), and γ_k is the spectral index after termination of effective acceleration. It is assumed that spectra are simple power laws with the index γ_k after termination of effective acceleration.

As later we will fit spectra of nuclear groups and the all particle spectrum, we convert rigidity spectra to spectra by energy per particle E .

$$I(E) = \frac{Q_p(R) \times \tau_{\text{esc}}(R)}{1 + \lambda_{\text{esc}}(R)/\lambda_p} \times \frac{dR}{dE} \quad (6)$$

$$R = \frac{1}{Z} \times \sqrt{E^2 + 2m_p \times A \times E};$$

$$\frac{dR}{dE} = \frac{1}{Z} \times \frac{E + m_p A}{\sqrt{E^2 + 2m_p \times A \times E}} \quad (7)$$

where Z and A are particle charge and atomic weight, and m_p is proton mass.

The spectrum of each cosmic ray nuclear group is the sum of spectra from the different classes of sources.

We described sources of class I with values of $\alpha = 2.3$ and $R_{\text{max}} = 50$ TV, and sources of class II with $\alpha = 2.1$ and $R_{\text{max}} = 4$ PV. The intensities for various cosmic ray groups were chosen to fit both the data of direct measurements and the data of EAS in the high energy region. The predictions of the model along with experimental data for cosmic ray groups and the all particle spectrum are shown in Figs. 1–3 with dashed lines (above 10^4 GeV this line follows the solid line, which is described in Sect. 5). The parameters of the model are shown in Tables 1 and 2.

Above 300 GeV the proton spectrum (Fig. 1) is fitted closely by the model. The steepening of the helium spectrum above 10 TeV is not as clear as for proton one, but the line does not contradict the experimental data. The RUNJOB data for helium are much lower than the data of ATIC-2 and JACEE. This also holds true for other groups of nuclei. In the region below ~ 300 GeV the model does not agree with the experimental data. An identical behavior is seen for the spectra of heavier nuclear groups shown in Fig. 2 and for the all-particle spectrum shown in Fig. 3. We will discuss this discrepancy in Sect. 5. The parameters for class II that determine the knee region were chosen to fit the experimental data of HEGRA-AIROBIC, KASCADE and TUNKA, while the data of CASA-BLANCA and DICE appear to be below the model line.

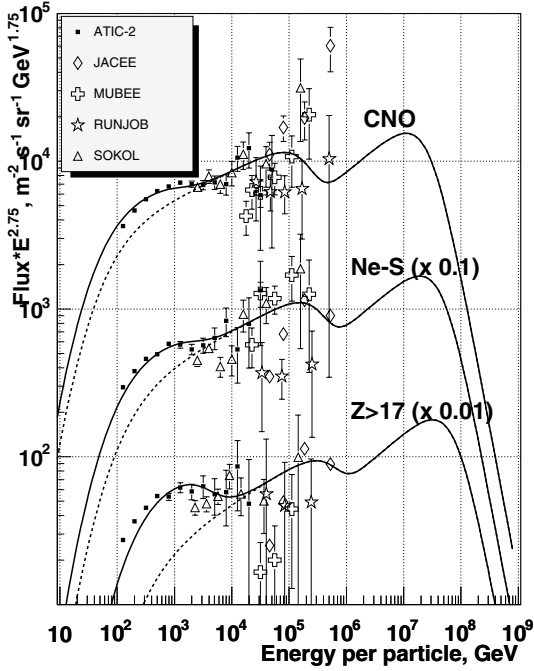


Fig. 2. Spectra of nuclear groups. Dashed lines are described in Sect. 3, solid lines are described in Sect. 5.

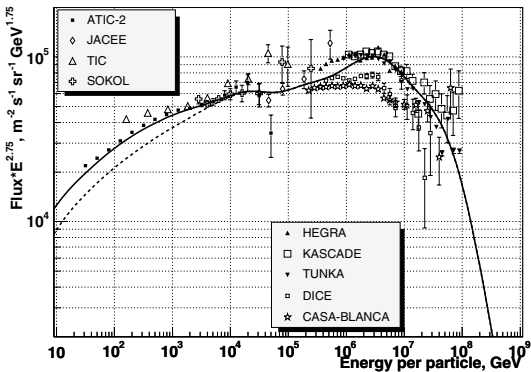


Fig. 3. All particle spectrum. The dashed line is described in Sect. 3, the solid line is described in Sect. 5.

4. Interpretation of the model

Our analysis is not the first attempt to link data of direct measurements with data of EAS and to fit the knee. Some previous models are phenomenological, e.g. the polygonato model of Hörandel (2003) and some are based on physical grounds. In a number of papers, the origin of the knee is explained by the structure of magnetic fields in the Galaxy, or the change of inelastic interaction characteristics above several PeV. Erlykin & Wolfendale (1997) assumed that the knee arises from a single nearby cosmic ray source. A detailed review of various models was made by Hörandel (2005).

As two classes of cosmic ray sources are needed for our model, we use the model of Bierman (1993) where two types of astrophysical objects are supposed as sources of the Galactic cosmic rays. The first type is stars with masses from 8 to 15 of solar mass that exploded into the interstellar medium (ISM). The expected chemical composition generated by these objects is close to the composition of the ISM. The second type is massive stars exploding into their own stellar wind. The stars of 15–25 solar masses known as Red Supergiants (RSG) possess

Table 2. Parameters for three classes of sources. Class I: SN into ISM; class II: SN in the Superbubble, class III: Novae.

Class	α	R_{\max} [GV]	γ	γ_k
I	2.3	5×10^4	2.63	8
II	2.1	4×10^6	2.43	4.5
III	2.57	2×10^2	2.9	4.5

Table 3. Flux $\times E^{2.75}$ [$\text{m}^{-2} \text{s}^{-1} \text{ster}^{-1} \text{GeV}^{1.75}$] for cosmic ray groups at $E = 10$ TeV.

	Z_{eff} (λ_p)	Flux $\times E^{2.75}$		
		class I	class II	class III
H	1(74)	1.4×10^4	6.25×10^3	0.6
He	2(18)	8.5×10^3	8.5×10^3	1.5
CNO	7(5.8)	6.75×10^3	1.8×10^3	30
Ne-S	12(3.5)	5.5×10^3	1.5×10^3	110
Z > 17	20(2.4)	3.5×10^3	1.2×10^3	750

a moderate stellar wind and the stars of mass greater than 25 solar masses known as Wolf-Rayet (WR) stars have a strong stellar wind. The wind stars are the late stage of evolution of massive O and B stars, which are clustered into OB associations. The combined effect of collective stellar winds and supernovae within OB associations leads to the production of a superbubble (Heiles 1979; Bruhweiler et al. 1980; Tomisaka 1992), i.e. a huge (several hundred parsec) region of hot ($\sim 10^6$ K), low-density ($\sim 10^{-3} \text{cm}^{-3}$) gas, surrounded by a cold neutral hydrogen supershell. It was supposed that the Sun is located within such a superbubble (Kafatos et al. 1981). It was shown (Kafatos et al. 1981; Streitmatter et al. 1985; Lingenfelter et al. 2000; Higdon & Lingenfelter 2003, 2005; Streitmatter & Jones 2005) that in this case many observed features of cosmic rays can be explained (age, anisotropy, some features of isotopic composition). We assume that our first class comes from the explosions of isolated stars into the ISM, and that our second class comes from supernovae within the local superbubble.

We assume that the second type of source generates cosmic rays with flatter spectra and with higher maximal energy. These are those cosmic rays that are studied by ground EAS arrays, and that produce the knee in the PeV energy region.

5. Energy spectra below ~ 300 GeV per nucleon

We now direct our attention to the energy region below ~ 300 GeV per nucleon. As one can see from Figs. 1–3 (dashed lines), the model with two classes of sources does not fit the preliminary ATIC-2 experimental data well. The weak reacceleration is unable to fit the spectra in the low energy region and it may be suggested that most of cosmic rays below 300 GeV per nucleon are accelerated in sources of a third class. The parameters for sources of the third class required to fit the experimental data are the following: $\alpha = 2.57$; $R_{\max} = 200$ GV; $\gamma_k = 4.5$. In the region of such low rigidities, the solar modulation must be taken into account. We have used the equation from Boezio (1997) for this purpose with modulation parameter $\Phi = 600$ MV.

$$\text{flux}_{\text{mod}}(E) = \text{flux}(E + Ze \times \Phi) \times P, \quad (8)$$

$$P = \frac{E^2 + 2m_p E}{(E + Ze \times \Phi)^2 + 2m_p(E + Ze \times \Phi)},$$

where e is the charge of the electron, m_p is the proton mass and E is the kinetic energy of the nucleus.

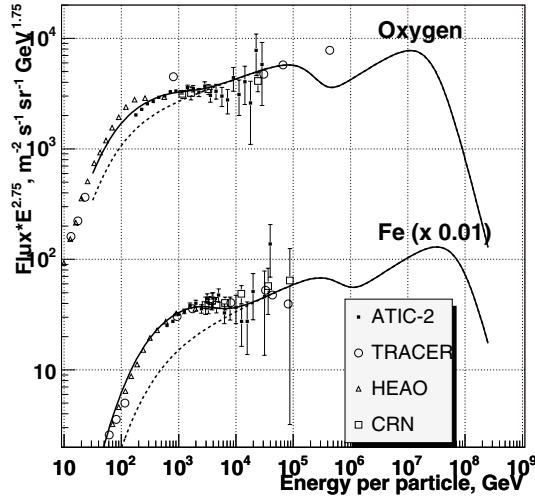


Fig. 4. Spectra of oxygen and iron.

The intensities for various cosmic ray components were chosen to fit the experimental data in Figs. 1–3. The fit in the version of model with three classes of sources is shown in Figs. 1–3 with solid lines.

To check our model in this low energy region we plot experimental data for separate heavy elements, oxygen and iron, obtained from HEAO-3-C2 (Engelmann et al. 1990), CRN (Müller et al. 1991), and preliminary TRACER results (Müller et al. 2005) and the preliminary ATIC-2 data (Panov et al. 2006) along with two versions of the model in Fig. 4. The model of three classes of sources fits the experimental data well. The model also fits other individual spectra.

Nova stars are candidates for the third class of sources. During nova explosion, an expanding shell is produced, and the broad features of nova explosion are similar to these of the explosion of supernovae. Power requirements are also satisfied: the mean energy of explosion is $W \sim 10^{46} - 10^{47}$ erg; the frequency of nova explosions is $\sim 100 \text{ year}^{-1}$ (Pskovskiy 2000). So, the power available for cosmic ray generation is:

$$\frac{(10^{46} - 10^{47}) \times 100}{3 \times 10^7} \approx 3 \times 10^{40} - 3 \times 10^{41} \text{ erg/s.}$$

It is not lower than the power supplied by supernova. Thus, this source class could generate cosmic rays with a steeper spectrum ($\alpha = 2.57$) and of significantly lower maximal rigidity (200 GV).

6. Parameters of the model, fluxes of different cosmic ray groups and $\langle \ln A \rangle$

The parameters of the model used to fit spectra of cosmic ray groups are shown in Tables 1 and 2. Figure 5 shows fluxes of cosmic ray groups and the mean value of $\langle \ln A \rangle$ in the model. The special feature of our model is that charge composition is not a monotonic function of energy: it becomes “lighter” before the knee, and only above the knee becomes heavier.

7. Conclusion

We proceed from the assumption that the difference between proton and helium spectral indices found in the JACEE experiment above 10 TeV (Asakimori et al. 1998), and supported by the preliminary ATIC-2 analysis (Wefel et al. 2005) in the energy

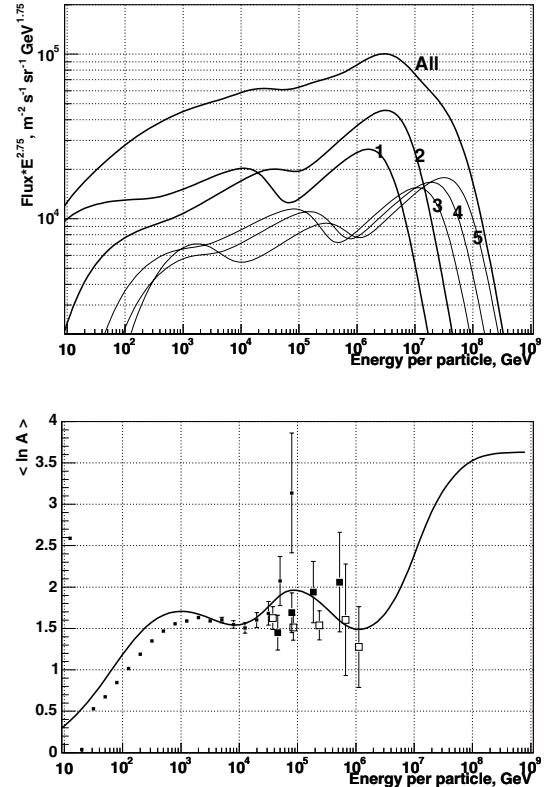


Fig. 5. Top panel: fluxes of cosmic ray groups in the model. Line numbers 1: protons, 2: helium, 3: CNO group, 4: Ne - S group, 5: Fe group ($Z > 17$). Bottom panel: $\langle \ln A \rangle$ vs. energy; small squares: preliminary ATIC-2, large solid squares: JACEE, open squares: RUNJOB.

region above 100 GeV is real. We suppose that this difference results from the fact that cosmic ray fluxes are a mixture of fluxes from sources with different spectral indices and different maximal energy. We checked a simplest model assuming two classes of sources. We showed that elemental cosmic ray spectra pointed to a “kink” at the rigidity of about 50 TV, and connected this with the assumption that one class of sources terminates its effective acceleration at this rigidity. This source class may be identified with the supernova explosions into the ISM. The second source class, presumably supernovae within the local superbubble, accelerates cosmic rays up to rigidity of 4 PV, producing the classic knee. However, the assumption of these two classes of sources is inadequate to fit the energy spectra below 300 GeV per nucleon along with the spectra in the high energy region, even taking into account minimal reacceleration of cosmic rays in the Galaxy. We assume that the contribution of nova stars is essential in the energy region below ~ 300 GeV per nucleon.

Acknowledgements. This work was supported by the Russian Foundation for Basic Research, grant number 05-02-16222. We are grateful to J.P. Wefel and T.G. Guzik for useful discussions.

References

- Adams, J., et al. 1997, Bull. Russ. Acad. Sci., 61, 1181
- Alcaraz, J., Alpat, B., Ambrosi, G., et al. 2000a, Phys. Lett. B, 490, 27
- Alcaraz, J., Alpat, B., Ambrosi, G., et al. 2000b, Phys. Lett. B, 494, 193
- Arqueros, F. 2000, A&A, 359, 682
- Asakimori, K., Burnett, T. H., Cherry, M. L., et al. 1998, ApJ, 502, 278
- Batkov, K. E., et al. 2005, Proc. 29 ICRC (Puna) 3, 353
- Boezio, M., Carlson, P., Francke, T., et al. 1997, ApJ, 487, 415

- Boezio, M., Bonvicini, V., Schiavon, P., et al. 2003, *Astropart. Phys.*, 19, 583
- Bierman, P. L. 1993, *A&A*, 271, 649
- Bruhweiler, F. C. 1980, *ApJ*, 238, L27
- Budnev, N. M., et al. 2005, *Proc. 29th ICRC (Puna)* 6, 257
- Derbina, V. A., Galkin, V. I., Hareyama, M., et al. 2005, *ApJ*, 628, L41
- Engelmann, J. J., et al. 1990, *A&A*, 233, 96
- Erlykin, A. D., & Wolfendale, A. W. 1997, *J. Phys. G.*, 23, 979
- Fowler, J. W., et al. 2000 [ArXiv:astro-ph/0003190] v2
- Haino, S., Ferrando, P., Soutoul, A., Goret, P., & Juliusson, E. 2004 [ArXiv:astro-ph/0403704]
- Heiles, C. 1979, *ApJ*, 229, 533
- Higdon, J. C., & Lingenfelter, R. E. 2003, *ApJ*, 590, 822
- Higdon, J. C., & Lingenfelter, R. E. 2005, *ApJ*, 628, 738
- Hörandel, J. R. 2003, *Astropart. Phys.*, 19, 193
- Hörandel, J. R. 2005 [ArXiv:astro-ph/0508014]
- Ivanenko, I. P., et al. 1993, *Proc. 23rd ICRC (Calgary)* 2, 17
- Kafatos, H., et al. 1981, *Proc. 17th ICRC (Paris)* 2, 222
- Kieda, D. B., et al. 1999, *Proc. 26th ICRC (Salt Lake City)* 3, 191
- Lingenfelter, R. E., Higdon, J. C., Ramaty, R., et al. 2000 [ArXiv:astro-ph/0004166]
- Müller, D., Swordy, S. P., Meyer, P., et al. 1991, *ApJ*, 374, 356
- Müller, D., et al. 2005, *Proc. 29th ICRC (Puna)* 3, 89
- Osborne, J. L., & Ptuskin, V. S. 1988, *Sov. Astron. Lett.* 14(2), 132
- Panov, A. D., Adams, J. H., Ahn, H. S., et al. 2006, *Adv. Sp. Res.*, 37, 1944
- Pskovskiy, Y. P. 1985, *Nova and supernova stars (Moscow: Nauka)*
- Roth, M., & Ulrich, H. 2003, *Proc. 28th ICRC (Tsukuba) Japan*, 1, 139
- Streitmatter, R. E., Balasubrahmanyam, V. K., Ormes, J. F., & Protheroe, R. J. 1985, *A&A*, 143, 249
- Streitmatter, R. E., & Jones, F. C. 2005, *Proc. 29th ICRC (Pune)* 3, 157
- Takahashi, Y., et al. 1998, *Nucl. Phys. B*, 60, 83
- Tomisaka, K. 1992, *Publ. Astron. Soc. Japan*, 44, 177
- Wefel, J. P., et al. 2005, in *Proc. 29 ICRC (Puna)* 3, 105
- Zatsepin, V. I., et al. 1993, *Proc. 23rd ICRC (Calgary)*, 2, 13
- Zatsepin, V. I., Lazareva, T. V., Sazhina, G. P., & Sokolskaya, N. V. 1994, *Phys. Atom. Nucl.*, 57, 645